Nanocomposite Polymer Electrolytes in PVDF/ZnO Membranes Modified with PVP for LiFePO_4 Batteries

Dyartanti, Endah R
Department of Chemical Engineering, Diponegoro University | Department of Chemical Engineering, Universitas Sebelas Maret

Widiasa, I Nyoman
Department of Chemical Engineering, Diponegoro University

Purwanto, Agus
Department of Chemical Engineering, Universitas Sebelas Maret

Susanto, Heru
Department of Chemical Engineering, Diponegoro University

https://doi.org/10.5109/1936213

出版情報：Evergreen. 5 (2), pp.19-25, 2018-06. 九州大学グリーンアジア国際リーダー教育センター
バージョン：

Nanocomposite Polymer Electrolytes in PVDF/ZnO Membranes Modified with PVP for use in $LiFePO_4$ Batteries

Endah R Dyartanti.[1,2*] I Nyoman Widiasa[1] Agus Purwanto[2] and Heru Susanto[1,*]

[1]Department of Chemical Engineering, Diponegoro University, Semarang, Indonesia

[2]Department of Chemical Engineering, Universitas Sebelas Maret, Surakarta, Indonesia

*Author to whom correspondence should be addressed,
Diponegoro University, Jl Prof Sudarto-Tembalang, Semarang 50275, Indonesia,
Telp.: +62247460058, Fax.: +62247480675,
E-mail: endah_rd@uns.ac.id
heru.susanto@che.undip.ac.id

(Received February 13, 2018; accepted June 4, 2018).

Polyvinylidene Fluoride/Zinc Oxide (PVDF/ZnO) nanocomposite membranes electrolytes were prepared via non-solvent induced phase separation (NIPS) method. used N,N-dimethyl acetamide (DMAc) as a solvent to dissolve the polymer (PVDF) so that different concentrations (–0, 4,5,6, 7and 8 wt. %) of polyvinylpyrrolidone (PVP) as pore-forming agents. and zinc oxide (ZnO) as filler. The as-prepared membranes were immersed in a coagulating bath containing a non-solvent (water) to complete the membrane pore structure. Scanning electron microscope (SEM) and Fourier transform infrared (FTIR) spectroscopy were used to characterize the structure and morphology of the membranes. Both the uptake of electrolyte and ionic conductivity of the membranes gel polymer electrolytes (GPEs) were increased with increases in the PVP content. The highest conductivity at room temperature for GPEs is found to be 5.64 mS cm-1. Additionally, the membrane's crystallinity (11.9 %) proved to be less than pure PVDF (37.26%), and a decrease in the crystallinity was detected with increases in the addition of PVP. A $LiFePO_4$ cathode was used to examine the performance of the GPEs in battery lithium-ion, and this discharge capacity of the gel-type composite membrane could be enhanced from 96.99 (PVDF) to 125.845 mA H g-1 (modified PVDF with ZnO and PVP) . The results suggest that this membranes gel electrolytes exhibited good feasibility to be used in large-capacity lithium-ion batteries that require high safety.

Keywords: PVDF; Polymer Gel Electrolytes; ZnO; PVP

1. Introduction

Nanocomposite gel polymer electrolytes (GPEs) are a unique category of polymer-based electrolytes that confer excellent ionic conductivity during liquid electrolyte replacement. These electrolytes are suitable for energy storage applications such as secondary batteries, fuel cells, and supercapacitors.[1)] GPEs are semi-solid electrolytes that integrate the advantages of both liquid and solid electrolytes. Compared with liquid electrolytes, this polymer version has convenient features that include a high level of ionic conductivity, enhanced safety, and less reactivity. In addition, these polymers are leakage proof with excellent dimensional stability, flexibility, and interface stability.[2,3)]

GPEs consist of a polymer matrix, entrapped liquid electrolytes, and suitable additives.[4)] Until now, Poly(vinylidene fluoride) (PVDF), poly (vinylidene fluoride-hexafluoropropylene),[4,5)] (poly (ethylene oxide) (PEO), polyacrylonitrile (PAN), and poly (methyl methacrylate)) (PMMA) have been used as the host polymer matrix for GPE membranes.[6)] Due to its properties, PVDF has been used as the polymer matrix for lithium-ion battery membrane separation. The combination of a high electron-withdrawing functional group (–C–F) and a high dielectric constant (ε = 8.4) confers a high degree of electrochemical stability to PVDF-based membranes, which enhances the dissolution of lithium in electrolytes and increases the content of charge carriers.[7)]

Phase separation is a popular technology that is used to fabricate porous membranes for lithium-ion battery (LIB) polymer electrolytes.[8)] The pores of nanocomposite membranes are constructed using the phase-inversion technique to capture and retain a significant amount of liquid electrolytes, which enhances the conductivity of lithium ions.[9–11)]

Nevertheless, this pore structure and electrolyte uptake diminishes the mechanical characteristic of the membranes. Studies have shown that a polymer matrix with fillers greatly improves the ionic conductivity, the stability membranes dimension, the thermal stability, the discharge capacity, and the interfacial properties between polymer electrolyte–electrodes.[12–14]. The addition of inorganic nanoparticles such as ZrO_2, [15] TiO_2,[16] MgO,[17] Al_2O_3,[18] and SiO_2[8] improves the characteristic and performance of the polymer membranes, and increases the balance of the electrolytes facing lithium metal electrodes.[19] Rajasudha, et al.[20] explored the effect that ZnO fillers exert on PVDF-HFP+$LiClO_4$ nanocomposite membranes. A decrease in the crystallinity of the PVDF-HFP polymer matrix was observed. Also, an increase in the ionic conductivity of the polymer electrolytes was reported. Recently, Hashmi et al.[6] showed improvements in the ionic conductivity and in the thermal and electrochemical stability of a dispersion of zinc oxide (ZnO) nanoparticles in GPEs. The GPEs combined the benefits of nanoparticles with a pore-forming agent. Liu and his co-workers used a phase-inversion technique to investigate the effect of graphene in PVDF/graphene polymer electrolytes. The filler (graphene) enhanced the porosity and reduced the crystallinity of the membranes, which increased the electrolyte retention in PVDF/graphene nanocomposites.[21]

The nano-composite membranes used to retain the liquid electrolyte require micropores that are joined. Therefore, some researchers have modified the surface morphology of the membranes by introducing pore-forming agents. The use of a pore-forming agent in the GPEs nanocomposite membrane promoted the conductivity of lithium ions by improving the porosity of the membranes.[22] Poly(ethylene glycol) (PEG),[23] salicylic acid,[24] Polyvinylpyrrolidone (PVP), [25,26] and urea[11,22] are common pore-forming agents for improving the characteristics and performance of nanocomposite GPEs for secondary lithium batteries.

Although some researchers have recently used ZnO to prepare polymer electrolyte membranes,[6,27–29] to the best of our knowledge, the influence of PVP on the morphology and electrochemical performance of GPE-based polyvinylidene fluoride (PVDF)/Zinc Oxide (ZnO) nanoparticles has not been reported. In view of this, we attempted to investigate the effect of the addition of PVP (25 kDa) as a pore-forming agent on polymer electrolytes in lithium-ion batteries. As described in our previous work, the as-prepared membrane-based, PVDF and other nanofillers (PVDF / nano clay) with PVP 7 wt% improves the nanocomposite characteristics and performance of NPE membranes.[30] In the present work, modifications to the structure and electrochemical performance, as well as the ionic conductivity and battery performance of the PVDF/ZnO membranes, are further explored. This outstanding membrane is also applied to provide polymer electrolytes for Lithium-Ions Batteries ($LiFePO_4$-cathode).

2. Experimental

2.1 Material

PVDF (Sigma Aldrich, Mw 534,000), Polyvinylpyrrolidone (PVP) (MW 25,000), and N, N-dimethylacetamide (DMAc) were purchased from Merck. , nano ZnO (purchased from MTI, Corp) was used as a filler. The electrolyte solution was lithium hexafluorophosphate ($LiPF_6$) in ethylene carbonate (EC) / dimethyl carbonate (DMC) / Diethyl carbonate (DEC) (4:2:4 by volume) 1 Molar. (MTI Corp.). [31].

2.2 Preparation of the PVDF/PVP/ ZnO polymer electrolyte

A DMAc/ZnO solution was homogenized. Briefly, 0.4 g of ZnO was dispersed in 50 g of DMAc with stirring for 15 min. The solution was then preserved using an ultrasonic sonicator to obtain a homogenous solution. Then, 5 g of PVDF and 0.35 g of PVP were dissolved in a ZnO/DMAc dispersion. The solution was stirred continuously at 40 ^oC for 24 h followed by ultrasonic treatment for 2 h at 25 ^oC. The solution was allowed to de-foam for 10 h. The mixture was cast on a glass plate with 150 μm-thick adjusted using an adjustable film coater (Doctor Blade - MSK-AFA-II, MTI Corp). The nascent membranes were exposed to air for 10 s and dipped in a coagulation bath for 48 h to eliminate excess PVP and DMAc. Finally, the membranes were dried under a vacuum for 12 h (70 ^oC) to remove the remaining water and solvent.

2.3 Membrane Characterization.

The morphologies of the polymer membranes were visualized using a scanning electronic micrograph (SEM), FEI Inspect S50, after gold-palladium (180s) was sputtered onto the surface of the polymer membranes. The membrane's cross-section was observed after the samples were broken in liquid nitrogen. The crystallinity of the polymer electrolytes was investigated via X-ray diffraction (X-Ray Diffraction Rigaku Miniflex 600). The porosity of the nanocomposites was determined by dipping the membrane into n-butanol for 2 h then wiping both membrane surfaces with very soft tissue paper. Furthermore, the membrane was weighed to determine the mass of absorbed n-butanol. The porosity (P) was determined using the following equation:

$$P\ (\%) = \frac{M_{BuOH}/\rho_{BuOH}}{M_{BuOH}/\rho_{BuOH} + M_p/\rho_P} \times 100 \qquad (1)$$

In equation (1), M_m and M_{BuOH} are the mass of dry membranes and the mass of n-butanol adsorbed by the membrane, respectively, and ρ_{BuOH} and ρ_P are the n-butanol and polymer densities, respectively. [32] The mean porosity of each membrane was based on the average of

three membrane samples. The electrolyte uptake was determined in a simple glove box using equation (2). The membrane was cut into a disk, then weighed and immersed in an electrolyte solution (1 M $LiPF_6$ in EC/DMC/DEC (4:2:4 by volume) for 2 h. Both membrane surfaces were then wiped with a very soft tissue paper. The weight of the wet membrane was measured and dried in an oven at a temperature of 70 °C. The electrolyte absorbed was determined using equation (2), where M_0 and M are the mass of the dry membrane and the wet membrane, respectively.

$$\delta\,(\%) \;=\; \frac{M - M_0}{M_0}\; x\; 100\,\% \qquad (2)$$

Differential scanning calorimetry (Perkin Elmer DSC-7) was used to investigate the thermal properties of the membrane at temperatures of 20-350 °C with the heating elevated 10 °C per min^{-1}. The crystalline properties of the polymer electrolytes were observed via thermogravimetric analysis (STA Linseis Platinum Series) at heating rates of 10 °C min^{-1} from room temperature to 600 °C under a N_2 atmosphere. The membrane crystallinity was computed from the DSC data using equation (3).

$$X_C\,\% \;=\; \frac{\Delta H_{m\,sampel}}{\Delta H_m^{\star}}\; x\; 100 \qquad (3)$$

In equation (3), Xc is the crystallinity, $\Delta H_{m\,sampel}$ is the fusion enthalpy of the polymer, and $\Delta H_m^{\star}$ is the fusion enthalpy of totally crystalline PVDF, which is 104:7 J g^{-1}.

2.4 Electrochemical and battery performance

Electrochemical evaluation was performed by dipping a membrane sample (area ~ 2 cm^2) into the electrolyte solution – 1 M lithium hexafluorophosphate ($LiPF_6$) in a (EC):(DMC):(DEC) (4:2:4 by volume) mixture. The samples were sandwiched between SS blocking electrodes in CR2032 coin cell cases. The ionic conductivity measurements were conducted using a HIOKI LCR Hi-Tester Model 3532 for frequencies ranging from 42 Hz to 5 MHz at an amplitude of 10 mV. Moreover, the ionic conductivity was determined using equation (4).

$$\sigma \;=\; \frac{d}{R_b\, S} \qquad (4)$$

In equation (4), R_b is the bulk resistance, σ is the ionic conductivity, and S and d are the area and the thickness of the specimen, respectively.

The coin cells (CR2032) were sandwiched in a glove box to evaluate the performance of the obtained Gels Polymer Electrolytes in a battery. The gel electrolyte was sandwiched between an anode and a cathode: Graphite (Anode)/ GPEs/ lithium iron phosphate ($LiFePO_4$) (cathode). The cells were placed in a charge/discharge Battery Analyzer (0.02 -10 mA, MTI corp.), and tested between 2.5 and 3.65 V under room temperature at a C-rate of 0.1.

3. Results and Discussions

3.1 Membrane chemistry

The membrane chemistry was observed using FTIR. The results are shown in Fig. 1. The characteristic peaks of PVDF were observed at 1414, 1233, 1176, and 881cm^{-1} and were assigned to the $–CH_2–$ deformation, [33] –C–F– stretching, –CF2– stretching, and to the amorphous band of PVDF, respectively.[34] The peaks of the α-phase were observed at 763 ($–CH_2–$ rocking) and 615 cm^{-1} ($–CF_2–$ bending and CCC skeletal bending). The peaks of the β-PVDF appeared at 840 cm^{-1} ($–CH_2–$ rocking and $–CF_2–$ stretching and 510 cm^{-1}. (CF_2)).[35] As depicted from Fig. 1, the intensity of the peaks at 763 and 615 cm^{-1} decreased as PVP loading increased, while the peaks of the β phase increased. Therefore, the FTIR results are in accordance with the results of the thermal characterization (changing of the crystal phase from α to β), which are discussed as follows. The complex formation was confirmed based on the above analysis.

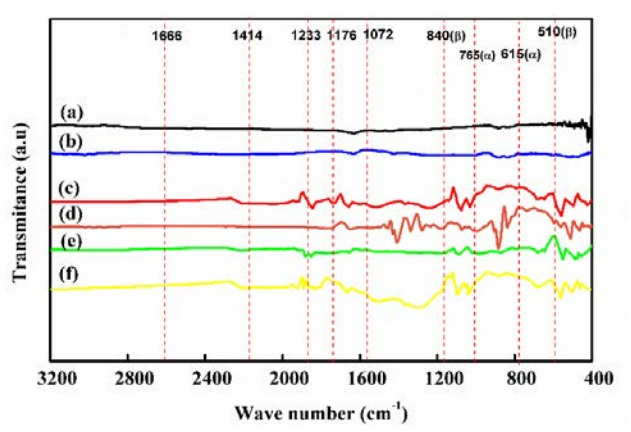

Fig. 1 FTIR spectra of GPEs: (a) Pure PVDF, (b) P-0, (c)P-4, (d) P-5, (e) P-7, and (f) P-8. For ZnO filler 8% weight.

3.2. Thermal Characterization

Thermal analysis and identification of the crystalline phases of PVDF were performed using Differential Scanning Calorimetry (DSC). The results are presented in Table 1. A change in the melting point (Tm) was observed with increasing nano-ZnO and PVP content. The melting point was slightly lower than that of PVDF/ZnO with PEG (Tm = 166.4°C).[36] The Crystallinities were based on the ΔHm data (104.7 J . g^{-1} ≈ 100% crystallinity) [37] and fell within a range of 11.97–37.26% for different PVP Concentrations. The contrasts in the high crystallinity were apparent when Graphene /DMAc solvent was applied with PVP as a pore-forming agent (44%).[21]

These crystallinity values were lower than when Acetone/DMAc was used as the solvent (40-38 %).[36] The reason is believed to be the solubility of PVP in DMAc solvent, which is higher than in Acetone/DMAc solvent. The increased pore-forming agent appeared to affect the modified PVDF/ZnO. Changing the crystal phase from α to β disrupted the arrangement of the nano-ZnO structure and led to a decrease in crystallinity.

Table 1. The melting point and crystallinity of PVDF/PVP/nano ZnO GPEs.

No	Sample	Degree of Crystallinity X_C (%)	Melting Point Tm (^{O}C)
1	P - 0	37.26	162.71
2	P - 4	32.84	163.34
3	P - 5	23.05	164.03
4	P - 6	11.97	165.87
5	P - 7	21.80	164.72
6	P - 8	31.36	164.12

Fig. 2 presents the TG curves. All membranes exhibited a small weight loss of approximately 2% up to 100 °C in the PVDF/ZnO system. The water content in the membranes could have contributed to this phenomenon.

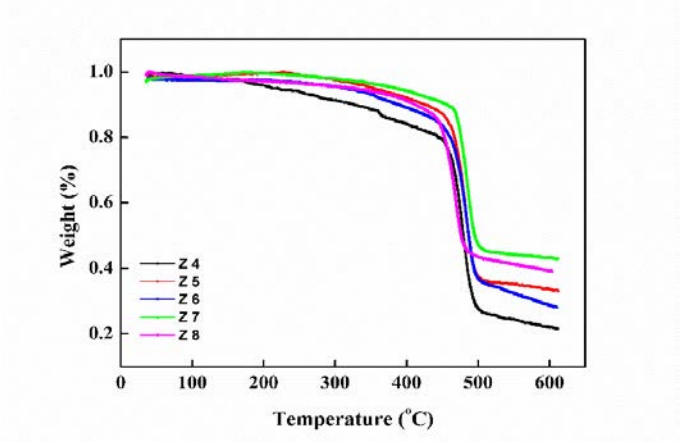

Fig 2. TG curve of modified PVDF/ZnO nanocomposites membranes with different PVP concentration

Between temperatures of 100 and 400 °C no weight loss was observed. This suggests that the membranes had excellent thermal stability. The thermal stability rose gradually with increases in the PVP content of up to 6% wt/wt. Interestingly, all modified PVDF/ZnO systems were thermally stable with no apparent weight loss up to 200 °C, which, from the standpoint of thermal stability, should make them suitable as polymer electrolytes in lithium batteries when using $LiFePO_4$ as a cathode.

3.3 Porosity and Electrolyte uptake

Fig. 3 shows the uptake of an electrolyte solution as a function of the PVP content and time, while Fig. 4 shows the relationship between porosity and the electrolyte uptake of nanocomposite membranes as a function of PVP content. The highest porosity for these membranes was 89.74% (prepared using nano ZnO 8 wt%; PVP 7 wt%). Hong and He[29] studied the effect of ZnO dispersed on a PVDF/PEG membrane and recorded a porosity of 75.15%, which was lower than the porosity obtained in this study. The higher porosity can be credited to the good hydrophilicity and water solubility of PVP, which is usually applied as a pore-forming agent to engineer the structure of PVDF nanocomposites. PVP could also work as a pore modifier to enhance the surface hydrophilicity so that a better amorphous phase through Lewis acid-base interactions is obtained. As a consequence, more free Li ions could be released, and a better transference of charge carriers was achieved to enhance the conductivity of the Lithium Ions.

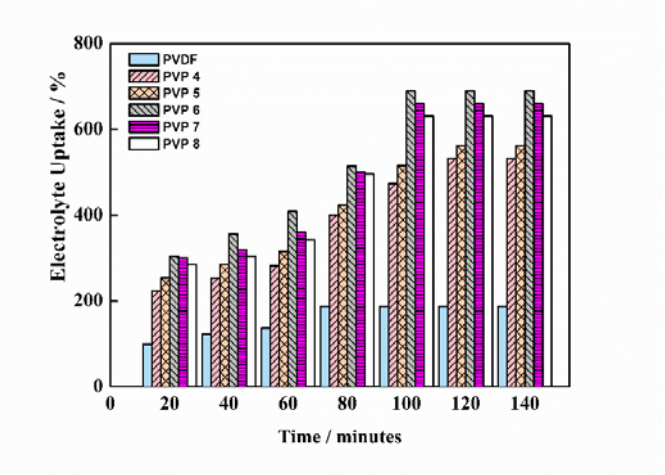

Fig. 3 Electrolyte uptake (%) of the PVDF/PVP/nano ZnO membranes with different PVP content.

The porosity and pore distribution is an essential factor in the electrolyte uptake of the GPEs. The highest electrolyte uptake was 689% (membrane with nano ZnO 8 wt%; PVP 6 wt%). Compared with a pure PVDF membrane reported by Deka and Kumar (263%)[38] and the PVDF membrane with dispersed graphene and PVP additive (470 %) reported by Liu et. al.,[21] this electrolyte uptake was significantly higher.

The main reason for this improvement is the addition of ZnO and PVP in PVDF, which generates more than 32.74% porosity. Another reason is the configuration of a more amorphous structure in the modified PVDF/ZnO compared with that in pure PVDF. It can be concluded that the electrolytes are caught in the extra pores in the amorphous phase of the polymer host, which would provide the additional 503% enhancement in liquid uptake. The co-effect of nano ZnO and PVP would contribute to an improvement in the electrolyte uptake.[39]

3.4 Ionic Conductivity

One of the essential characteristics of GPEs for

application as a LIBs separator is ionic conductivity. In this work, the effect of PVP on the ionic conductivity of GPEs was observed. The results are depicted in Fig. 4. As shown, the maximum conductivity of Li^+ ions was about 5.64 mS cm^{-1} at 8 wt% nano ZnO and 6 wt% PVP loading.

Addition of ZnO nanofiller and a PVP pore-forming agent was useful for enhancing the ionic conductivity. The result was confirmed by the Porosity and electrolyte absorption, which were both increased in the Polymer matrix, The ZnO increased the ionic conductivity by providing Li^+ conduction tunnels through Lewis acid-base interactions.[22] Furthermore, the oxygen-containing functional groups in the surface region of the ZnO enhanced the lithium ion migration. Moreover, the excessive PVP in the polymer electrolyte promoted aggregation leading to a decrease in the volume of the interface layer. Consequently, the ionic conductivity was reduced with further increases in PVP into the polymer electrolytes.

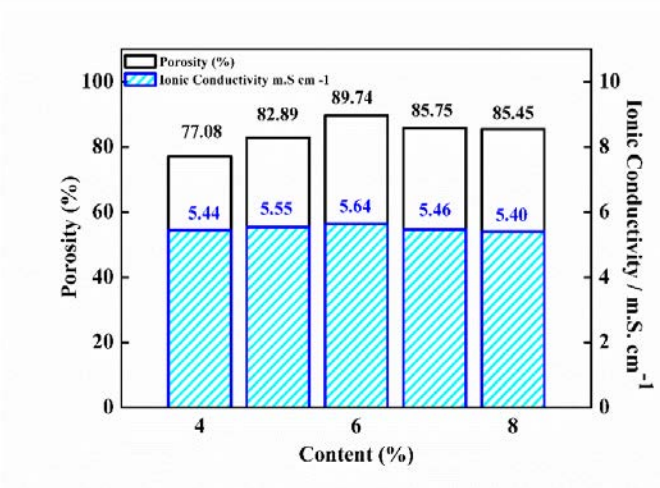

Fig. 4 Ionic Conductivity of the PVDF membranes with different content of (a) ZnO at 7 wt% PVP and (b) PVP at 8 wt% nano ZnO.

The enhanced ionic conductivity of GPES by the addition of pore-forming agents was also described in previous studies.[20,21] However, introducing nano-ZnO into the PVDF membrane with PVP as a pore-forming agent exhibited ionic conductivity that was higher than either the GPES with SiO_2 and urea or graphene with PVP, as reported in earlier studies. Li et al. [22] reported that the ionic conductivity of GPES with urea (pore forming agent) and 10% SiO_2 (filler) at 30 was 3.652 mS cm^{-1}. Liu et al. [21] reported ionic conductivity for GPES with PVP (as pore-forming agent) and 0.002% wt. graphene that was 3.61 mS cm^{-1}. Lewis acid-base interactions between the functional group's filler and polar group's electrolytes, the polymer chains, the filler and the crystallinity all play crucial roles in enhancing ion conductivity.

3.5 Battery Rate Performance

The cycle performance of a battery using the cell was analyzed using $LiFePO_4$ as the cathode, graphite as the anode, and an as-prepared membrane at a 0.1 C-rate with voltage limited to between 2.2 and 3.65 V at ambient temperature. Fig. 5 shows the discharge capacity and coulombic efficiency of the LiFePO4 battery and different GPEs. After 48 cycles, the average discharge capacity of the battery with modified PVDF (125.845 mA h g-1) was higher than the celgard separator (101 m A h g-1) and PVDF only (96.99 mA h g-1). Also, the initial discharge capacities of the as-prepared GPEs, celgard, and PVDF separator were 126.546, 100.3, and 97.119 mA h g-1, respectively. After 48 cycles, the final discharge capacities were 125.601, 101.126, and 97.015 mAh g-1. The values for fade in capacity per cycle of GPEs, Celgard, and pure PVDF were 0.02, 0.004, and 0.01 mA h g-1, respectively. Under continuous cycling, the leakage and decomposition of the electrolyte and loss of adhesion resulted in a capacity fade of the battery cell with GPEs. This better cycling performance indicates a low level of internal polarization, as explained by Li et al.[40] This low polarization is caused by excellent wettability and high ionic conductivity of the membrane separators. Furthermore, the porous structure, higher electrolyte absorption, and excellent compatibility with cathodes and anodes are another possible reason.

The rate capabilities of the battery cell under different charge/discharge rates were determined in order to verify battery reliability. Fig. 6 presents the rate capacities of cells with modified PVDF / ZnO membranes. Increasing the current rate decreases the specific capacities of batteries. The capacities of the tested battery showed the highest discharge capacity at 0.1 C. When the current rate was increased to 4 C, the PVDF membrane (pure) displayed poor capability. The discharge capacities of the cells with modified PVDF membranes, celgard, and pure PVDF were 60.887 (P-6), 35.672 (Celgard), and 31.192 (pure PVDF), respectively. The cells with the modified PVDF/ZnO composite membrane exhibited a better discharge capacity than the cells with the Celgard and pure PVDF. The better battery discharge capacity was evidenced by a porosity and ionic conductivity that was higher than both PVDF (only) and Celgard.

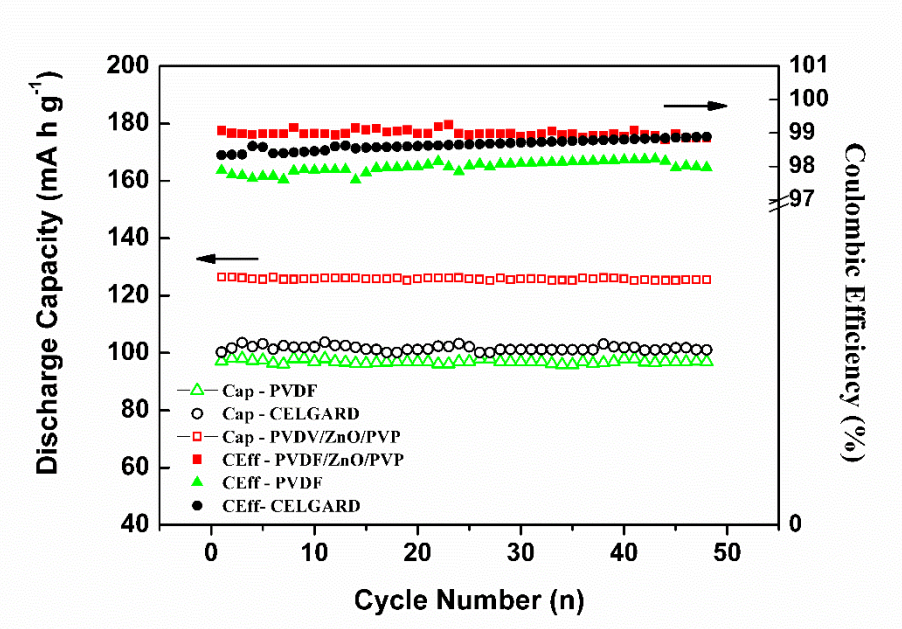

Fig 5. Discharge capacity and Coulombic Efficiency of the $LiFePO_4$ /GPES/ Graphite cells battery at 0.2 C rate

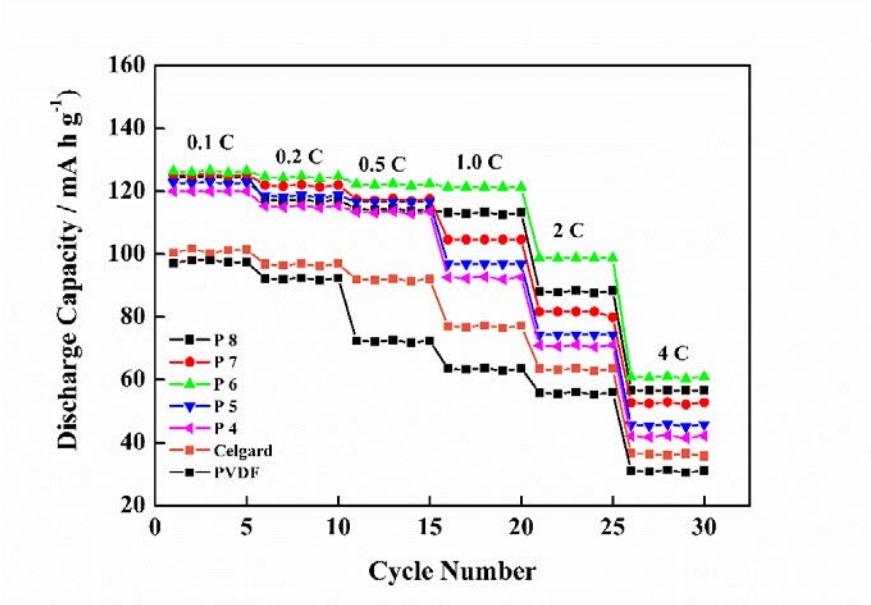

Fig 6. The discharge capacities of the $LiFePO_4$ battery with different GPEs

4. Conclusions

A nanocomposite membrane based on PVDF modified with PVP as a pore-forming agent and nanofiller (ZnO) was fabricated and characterized. The use of both PVP and nano ZnO on a PVDF membrane increased the presence of GPEs. This increases battery charge-discharge performance by enhancing membrane characteristics such as porosity, electrolyte uptake and ionic conductivity. The fabricated cell assembled with GPEs also displayed excellent discharge capacity. Thus, we believe that the modified PVDF/ZnO nanocomposites are promising material for use as polymer electrolytes in LIBs.

Acknowledgements

The authors are sincerely grateful for financial support from the Universitas Sebelas Maret for Hibah PNBP UNS -Penelitian Disertasi Doktor 2017 Grant number 1075/UN27.21/PP/2017, and for the doctoral scholarship program. The authors are grateful to The Center for Science and Technology Advanced Materials, National Nuclear Energy Agency Indonesia for assistance with the EIS studies and to smart city project by US-aid Shera for the opportunity given to increase the quality of this paper.

References

1). S.-U. Kim, D.M. Yu, T.-H. Kim, Y.T. Hong, S.Y. Nam, and J.-H. Choi, *J. Ind. Eng. Chem.* **23**, 316 (2015).

2). K. Chihara, M. Ito, A. Kitajou, and S. Okada, *Evergreen* **4**, 1 (2017).

3). K. Nakamoto, R. Sakamoto, A. Kitajou, M. Ito, and S. Okada, *Evergreen* **4**, 6 (2017).

4). M. Yang and J. Hou, *Membranes (Basel).* **2**, 367 (2012).

5). H. Lee, M. Yanilmaz, O. Toprakci, K. Fu, and X. Zhang, *Energy Environ. Sci.* **7**, 3857 (2014).

6). S.A. Hashmi, J. Solid State Electrochem. **16**, 3105 (2012).

7). A.M. Stephan, *Eur. Polym. J.* **42**, 21 (2006).

8). Y. Li, X. Li, H. Guo, Z. Wang, and T. Li, Iran. *Polym. J.* **23**, 487 (2014).

9). Z. Chen, L.Z. Zhang, R. West, and K. Amine, *Electrochim. Acta* **53**, 3262 (2008).

10). W.H. Pu, X.M. He, L. Wang, C.Y. Jiang, and C.R. Wan, *J. Membr. Sci.* **272**, 11 (2006).

11). W. Xiao, C. Miao, X. Yin, Y. Zheng, M. Tian, H. Li, and P. Mei, *J. Power Sources* **252**, 14 (2014).

12). J. Chen, S. Wang, D. Cai, and H. Wang, *J. Memb. Sci.* **449**, 169 (2014).

13). H.-S. Jeong, S.C. Hong, and S.-Y. Lee, *J. Memb. Sci.* **364**, 177 (2010).

14). J. Cao, L. Wang, M. Fang, X. He, J. Li, J. Gao, L. Deng, J. Wang, and H. Chen, *J. Power Sources* **246**, 499 (2014).

15). W. Xiao, X. Li, Z. Wang, and H. Guo, *Iran. Polym. J.* **21**, 481 (2012).

16). J. Cao, L. Wang, Y. Shang, M. Fang, L. Deng, J. Gao, J. Li, H. Chen, and X. He, *Electrochim. Acta* **111**, 674 (2013).

17). R. Kumar, A. Subramania, N.T.K. Sundaram, G.V. Kumar, and I. Baskaran, *J. Memb. Sci.* **300**, 104 (2007).

18). Z. Li, G. Su, D. Gao, X. Wang, and X. Li, *Electrochim. Acta* **49**, 4633 (2004).

19). X.M. He, Q. Shi, X. Zhou, C.R. Wan, and C.Y. Jiang, *Electrochim. Acta* **51**, 1069 (2005).

20). G. Rajasudha, H. Shankar, P. Thangadurai, N. Boukos, V. Narayanan, and A. Stephen, *Ionics (Kiel).* **16**, 839 (2010).

21). J. Liu, X. Wu, J. He, J. Li, and Y. Lai, *Electrochim. Acta* **235**, 500 (2017).

22). Y. Li, W. Xiao, X. Li, C. Miao, H. Guo, and Z. Wang, *Ionics (Kiel).* **20**, 1217 (2014).

23). Y. Li, J. Wang, J. Tang, Y. Liu, and Y. He, *J. Power Sources* **187**, 305 (2009).

24). H.P. Zhang, P. Zhang, G.C. Li, Y.P. Wu, and D.L. Sun, *J. Power Sources* **189**, 594 (2009).

25). C.V.S. Rao, M. Ravi, V. Raja, P.B. Bhargav, A.K. Sharma, and V.V.R.N. Rao, *Iran. Polym. J.* **21**, 531 (2012).

26). C.-Y. Chiu, Y.-J. Yen, S.-W. Kuo, H.-W. Chen, and F.-C. Chang, *Polymer (Guildf).* **48**, 1329 (2007).

27). O. Padmaraj, M. Venkateswarlu, and N. Satyanarayana, *Ionics (Kiel).* **19**, 1835 (2013).

28). E.M. Masoud, M.E. Hassan, S.E. Wahdaan, S.R. Elsayed, and S.A. Elsayed, *Polym. Test.* **56**, 277 (2016).

29). J. Hong and Y. He, *Desalination* **302**, 71 (2012).

30). E.R. Dyartanti, A. Purwanto, I.N. Widiasa, and H. Susanto, *AIP Conf. Proc.* **1710**, 1 (2016).

31). E.R. Dyartanti, H. Susanto, I.N. Widiasa, and A. Purwanto, in *IOP Conf. Ser. Mater. Sci. Eng.* (IOP Publishing, 2017), p. 12052.

32). P. Raghavan, X. Zhao, J.-K. Kim, J. Manuel, G.S. Chauhan, J.-H. Ahn, and C. Nah, *Electrochim. Acta* **54**, 228 (2008).

33). S. Rajendran, O. Mahendran, and R. Kannan, *Mater. Chem. Phys.* **74**, 52 (2002).

34). D. Saikia and A. Kumar, *Electrochim. Acta* **49**, 2581 (2004).

35). S. Rajendran, O. Mahendran, and T. Mahalingam, *Eur. Polym. J.* **38**, 49 (2002).

36). R. Prasanth, N. Shubha, H.H. Hng, and M. Srinivasan, *Eur. Polym. J.* **49**, 307 (2013).

37). Y. Rosenberg, A. Siegmann, M. Narkis, and S. Shkolnik, *J. Appl. Polym. Sci.* **43**, 535 (1991).

38). M. Deka and A. Kumar, *J. Power Sources* **196**, 1358 (2011).

39). J. Cao, L. Wang, M. Fang, X. He, J. Li, J. Gao, L. Deng, J. Wang, and H. Chen, *J. Power Sources* **246**, 499 (2014).

40). S. Li, B. Li, X. Xu, X. Shi, Y. Zhao, L. Mao, and X. Cui, *J. Power Sources* **209**, 295 (2012).